Int J Adv Manuf Technol (2012) 58:1189–1199
DOI 10.1007/s00170-011-3443-y

ORIGINAL ARTICLE

Study on energy input and its influences on single-track, multi-track, and multi-layer in SLM

Wang Di · Yang Yongqiang · Su Xubin · Chen Yonghua

Received: 4 October 2010 / Accepted: 7 June 2011 / Published online: 30 June 2011

Abstract Energy input is crucial in the manufacturing of high-density metal part with smooth surface. In this article, the authors had studied the single-track, multi-track, and multi-layer and had obtained four types of typical tracks, including regular and thick shape, regular and thin shape, regular but occasionally broken shape, irregular and pre-balling shape. The analysis of single- and multi-track experiments showed that the regular and thin shape was the most suitable for selective laser melting (SLM) fabrication. Multi-track experiments proved that dense and smooth surface can be obtained when the overlapping rate was around 30% based on the regular- and thin-shaped track. As a result of the heat accumulation effect during multi-track and multi-layer fabrication, it was possible to obtain ideal track type with less energy input. In multi-layer experiment, the gradually thicken layer was the reason for the surface quality deterioration. The inter-layer stagger scanning strategy, which can improve the quality of the end-use part, was used in this experiment. By testing the 316 L stainless steel samples fabricated by the SLM process, the microstructure can be identified as composed of fine equiaxed and columnar grains, and the samples had higher tensile strength and hardness than castings of the same material, but with lower elongation. The experiments had proved that SLM process can directly produce high dense 316 L stainless steel part with smooth surface.

Keywords Selective laser melting · Energy input · Single track · Multi track · Multi layer · Density

W. Di · Y. Yongqiang (✉) · S. Xubin
School of Mechanical and Automotive Engineering,
South China University of Technology,
Guangzhou 510640, China
e-mail: meyqyang@scut.edu.cn

C. Yonghua
Department of Mechanical Engineering,
The University of Hong Kong,
Hong Kong, China

1 Introduction

Additive layer manufacturing is commonly used for manufacturing prototypes, tools, and functional end products (RM) in a wide range of industries including medicine, automotive, and aerospace industries [1–4]. One of the key advantages of RM over conventional manufacturing is the elimination of molds, dies, and other forms of tooling. Moreover, almost infinite geometrical complexity [5], individualization [6], and material flexibility [7] give RM more superior properties.

The selective laser melting (SLM) technique fully melts a predeposited layer of a single component metallic powder onto a substrate according to a computer-generated pattern, by successive powder deposition of these layers at 20–100 μm thickness. Directly after the production process, the manufactured parts or tools show a surface roughness between Ra 30–50 μm. By using laser resource to radiate powder to fabricate, full density parts can be difficult due to the formation of part porosity. The problems generally due to the high temperature and strong surface tension forces act on the melt, driving it towards a minimum surface energy rate, which is spherical, leaving areas of porosity between melt tracks [8]. High-temperature oxidation of the material, exacerbates the situation by further reducing wetting between melt beads [9]. High residual stresses are also generated in the layers causing curl.

So far, the researches on SLM have included the following aspects: fundamental theory [8–10], manufacturing process [6, 11–13], application fields [14, 15], and new materials research [16, 17], etc. The aims of these researches were to improve the density and solve the bad surface quality of the parts produced by SLM. In order to improve the density, many ways had been used including optimization of process parameters [9, 13], using special scanning strategies [12, 18], and so on. Most of the works highlighted on separate discussion about the impact of scanning speed, laser power, overlapping rate, and other process parameters on fabrication quality, while no one was associated the whole process of SLM and the heat accumulation effect. There were also many studies that had obtained good manufacturing results at absolutely different energy input conditions, but these studies did not well explain the energy requirements needed to directly fabricate metal parts by SLM method, and the definition of the energy input varied widely.

The main purpose of this article was to explore the procedure of obtaining high-density metal parts with smooth surface by SLM process. The research method was by the progressive study of single-track→multi-track→multi-layer, also taking energy input as the clue to (1) discuss the relationship between energy input and single track, and analyze the forming characteristics of single track; (2) study the overlapping rate between tracks by multi-track experiment; (3) analyze the influence of heat accumulative effect on parameters choice during the experiments; (4) choose scanning strategy and explain why the surface quality gradually getting worse; and (5) observe the microstructure and test the mechanical properties of 316 L stainless steel samples produced by SLM. Finally, typical application examples from the SLM technology were given.

This article will systematically analyze the process of fabrication of high-density metal parts by SLM method. Taking the energy input as the main clue to study on single-track, multi-track, and multi-layer fabrication, which gives a clear route for directly fabricate high-density metal parts by SLM.

2 Experiment procedure

2.1 SLM machine

The apparatus used was a self-developed Dimetal-280, which was a precommercial SLM workstation with a maximum laser power 200 W continuous wavelength of 1,090 nm Ytterbium fiber laser. The building envelop was 280×280×240 mm. The scanning system used was a Dual Axis Mirror Positioning System and a Galvanometer optical Scanner, which directs the laser beam in the *x*- and *y*-axis through an F-theta lens. The focusing optics was 163 mm focal length lenses, which produces a focused beam spot size of about 70 μm diameter. Since the powder was fully melted during the process, protection of the SLM-processed parts from oxidation is essential; therefore, all metal powder processing occurred in an argon or nitrogen atmosphere with no more than 0.15%. For the given laser parameters, the optimum thickness of the powder layer spread by scraper is 20–50 μm. Thicker layer is not desirable, as it leads to formation of droplets and, thus, to considerable deterioration of product quality. Figure 1 shows the schematic diagram of the operating principle of Dimetal-280 equipment.

2.2 Material

Gas atomized 316 L stainless steel powder was used in this experiment. The 316 L stainless steel is considered to be biocompatible and corrosion resistant. The main reason for selecting 316 L stainless steel is for its relatively mature research and its wide applications. The chemical composition and property of powder is shown in Table 1.

2.3 Experiment detail

Multi-layered part is built from multi single layers, and a single layer is composed of multi single tracks. Therefore, it is critical to fully understand and resolve problems within single-track and single-layer fabrication before progressing onto multi-layer fabrication. Basically, laser energy input controlling is key to affect the fabricated part quality, and its value determines the state of the molten powder, including vaporization state, melting state, and sintering state.

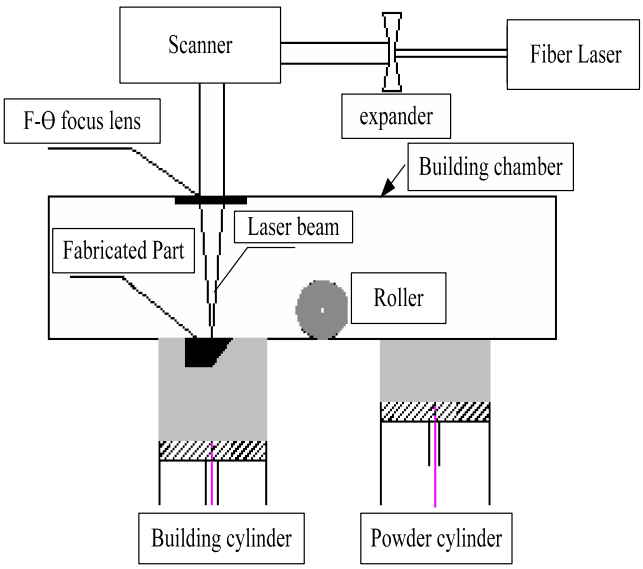

Fig. 1 The operating principle of SLM equipment

Table 1 Chemical compositions and property of 316 L stainless steel

Chemical composition (mass fraction)/%								Grain size distribution (mass fraction)/%				Apparent density/ (g cm^{-3})
C	Cr	Ni	Mo	Si	Fe	Mn	O	0–5.18 μm	5.18–15.15 μm	15.15–30.8 μm	Mean diameter	4.04
0.03	17.53	12.06	2.16	0.86	Bal	0.38	0.13	10	40	50	17.11	

Therefore, energy input will be taken as the main clue to optimize single track, the overlapping rate in multi-track experiment and scanning strategy in multi-layer process. The influence of heat accumulative effect on parameters optimization during multi-track and multi-layer fabrication will be discussed. Finally, cubic samples would be fabricated using optimized parameters by SLM. Density was taken as the core indicator to discuss the influence of processing parameters on density and surface morphology, and microstructure of the samples were analyzed. The mechanical properties and hardness were also tested for comparison with casting parts.

The relative density of the sample was calculated by $P/P_0 \times 100\%$, P_0 is the theoretical density of 316 L stainless steel, the actual density P of SLM fabricated samples were measured by Archimedes method. The sample was polished and etched before microstructure was observed; the etching liquid was composed of 5 g Fe_3Cl, 50 mL HCL and 100 mL deionized water. The surfaces of the specimens were observed under stereo-microscope and a scanning electron microscope. Micro-hardness and mechanical properties were measured respectively on Digital Micro-hardness tester HVS-1000 and Electronic Universal Testing Machine CMT5105.

3 Result and discussion

3.1 Single-track fabrication

The processing region in which the material would fully fuse was initially investigated by single-track experiment. The single-track investigation allows for identification of optimized processing parameters for laser power and scanning speed.

There are as many as 130 factors that affect the part's quality during SLM process [5], in which the key factors are around 20. In this experiment, the factors affecting the fabrication quality mainly including laser power, scanning speed, layer thickness, scanning spacing, spot diameter, scanning strategy, material properties (composition, particle size and shape, etc.), and inner-chamber environment (oxygen content, atmosphere humidity, etc.). Due to the layer thickness has significant influence on the stability of molten pool, which will tend to reduce the surface tension, easily leading to balling effect. Therefore, the layer thickness should be as thin as possible. In this experiment, layer thickness was set to 35 μm, which was decided by the powder particle size (the maximum particle diameter is about 25 μm). The laser spot diameter was 70 μm, and the material's physical properties are fixed parameters. Therefore, the main factors affecting the result of single-track experiment were laser power and scanning speed. Table 2 shows the process parameters of single-track experiment.

Four different types of tracks were obtained. It was found that the track type is closely related to the energy input per unit timeψ_1 (W cm^{-3}), which can be obtained by formula (1) [19]:

$$\psi_1 = \frac{4P}{\pi d^2 . v} \tag{1}$$

Where P is laser power, d is the spot diameter, and v is scanning speed. Different types of track can be got at different ψ_1 range.

1. As $\psi_1 > 2.6\times10^5$ W cm^{-3}, especially when scanning speed was rather low and laser power was high, for example P=150 W and v=50 mm/s, the shape of regular and thick track could be achieved as Fig. 2a shows.
2. As 1.3×10^5 W cm$^{-3} < \psi_1 < 2.6\times10^5$ W cm^{-3}, for example P=150 W, v=250 mm/s, the shape of regular and thin track could be achieved as Fig. 2b shows.
3. As 0.7×10^5 W cm$^{-3} < \psi_1 < 1.3\times10^5$ W cm^{-3}, for example P=100 W, v=280 mm/s, the shape of regular but occasionally broken track could be achieved as Fig. 2c shows.
4. As $\psi_1 < 0.7\times10^5$ W cm^{-3},especially when scanning speed was high and laser power was low, for example P=50 W, v=240 mm/s, track of irregular and preballing shape could be got, as Fig. 2d shows.

For the shape of regular and thick track, the high laser energy input would make the powder vaporize, which would reduce the material in the molten pool and blow

Table 2 The parameters of single track experiment

Laser power (W)	50	100	150
Scanning speed (mm/s) (step size. mm/s)	30–240 (30)	40–320 (40)	50–400 (50)

Layer thickness, 35 μm; oxygen content, ≤0.1%

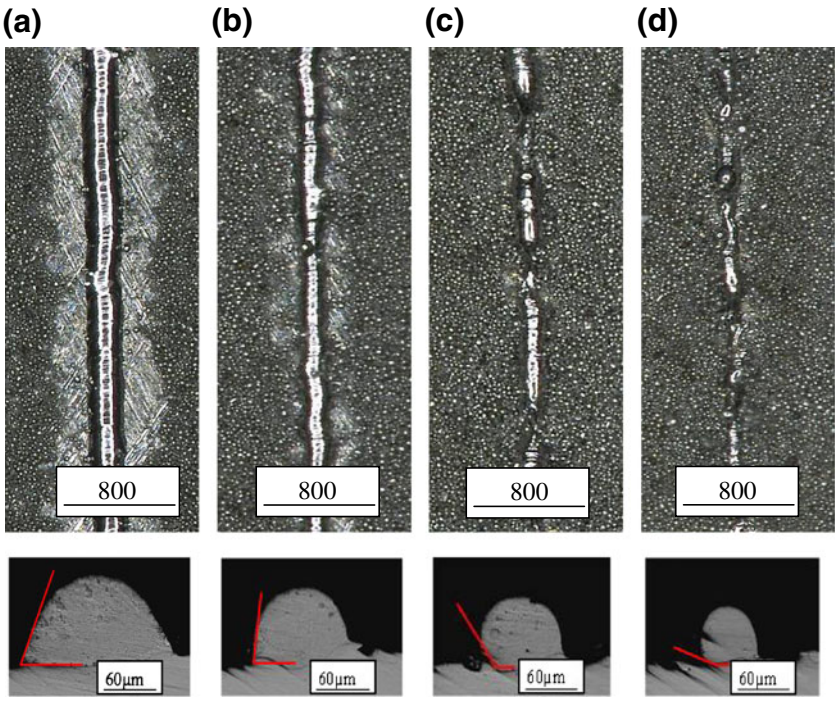

Fig. 2 Four typical track types and the corresponding cross sections

away the powder around the pool, so there was not enough powder remained for the next track. The higher the energy input, the larger the powder-free zone would be formed. The width of this type of tracks reached more than two times of the spot diameter.

For the shape of regular and thin track, the molten pool could not reach vaporization point and the pool's surrounding powder would not be blown away. The track was as regular and continuous as track above. The width of this type of tracks was between one and two times of the spot diameter.

As the energy input continued to fall, only near or in the center of the spot have enough energy to melt metal powder, track type of regular but occasionally broken shape was formed. The molten pool occasionally became irregular or noncontinuous. The track width was approximately equal to the spot diameter.

As energy input fell to a level incapable of melting enough powder, irregular and preballing shape track was formed, the track became much more irregular, the wetability was also very poor as the result of the not enough melting of the previous layer or the substrate plate. The track width was slightly bigger than half of the spot diameter for this type of track.

Figure 2 also shows the cross-sections of four types of track; it can be seen that the wetting angles of four types of track respectively are acute angle, nearly right angle, obtuse angle, and close to 180°. The smaller the wetting angle, the more helpful it will be for the SLM process. Therefore, the track of regular and thick shape and regular and thin shape are suitable for SLM process. Figure 3 shows the track shape distribution of single track based on experiments.

The above discussions of the four types of track have some differences compared to the results reported by other researchers. Yadroitsev [11] summarized the single-track types and divided them into three zones, including stability zone, instability zone, and drops formation zone. Childs [8] divided tracks into four types, including continuous with a

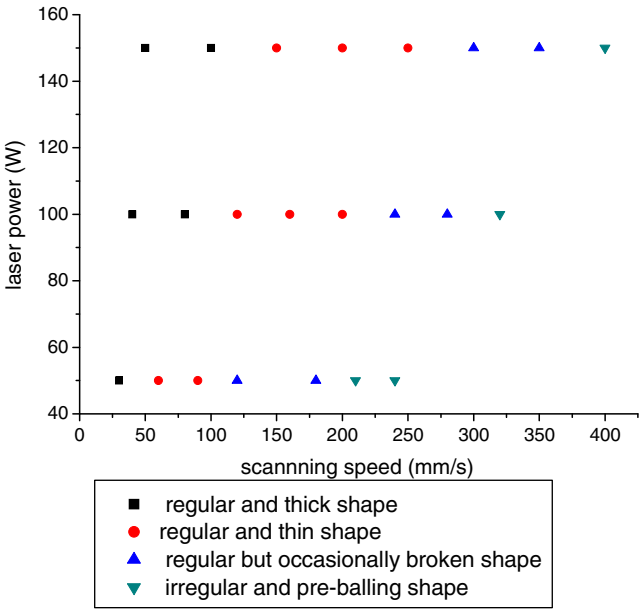

Fig. 3 Distribution of single-track types

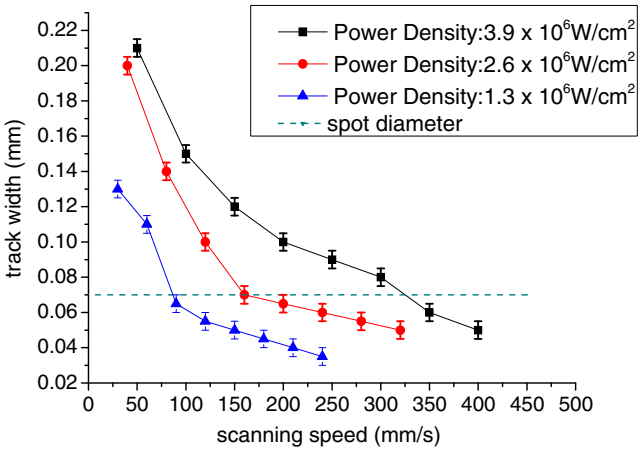

Fig. 4 The relationship between scanning speed, laser power density, and track width (layer thickness 35 μm)

crescent-shaped cross-section, continuous with an elliptic cross-section, irregularly broken, and balled or only partially melted. Compared with the above conclusion relevant to track types, serious balling phenomenon had not been found in authors' experiments. The reason may have much to do with the 35-μm layer thickness adopted in this experiment, while much thicker layer thickness was used by the aforementioned two researchers. The thinner layer thickness increases the stability of the molten pool, and the balling effect is hard to occur as the wetting ability between the molten pool and the substrate is improved. From single-track experiment, it is easy to obtain regular and continuous single track when the laser energy input is appropriate.

The boundaries of the energy input ψ_1 are not necessarily accurate for the division of four types of track. The single-track experiment provides a theoretical support for the multi-track and multi-layer experiments. Theoretically, a heat balance approach can be used to estimate if the energy radiated by laser would be sufficient to melt the powder as formula (2) [8]:

$$\frac{\alpha P}{v} = (c_p \times \Delta T + L) \times \rho \times V \tag{2}$$

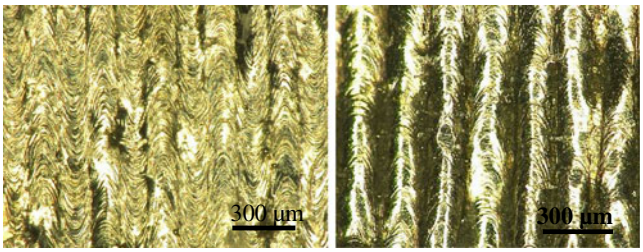

Overlapping rate 30% (scanning spacing 0.12mm)

Overlapping rate 10% (scanning spacing 0.16mm)

Fig. 6 Different overlapping rates experiment of the shape regular and thick track

In formula (2), α is energy absorption rate, c_p (kJ · kg^{-1}.°K^{-1}) is the specific heat, ΔT(°K) is the temperature rise needed for melting, L (KJ · kg^{-1}) is the latent melt energy, ρ (kg · mm^{-3}) the density and V the volume of the spherical particle. The equation will determine whether any particle absorbs enough energy to melt. The value calculated from this equation depends on all the material contributing to the volume V.

In this work, however, it is necessary to consider the energy absorption rate α and track mass m; α is associated with powder density, surface condition after deposition by blade or scraper; also, it is determined by laser wavelength. Different researchers had got absolutely different α value. The track mass m is hard to calculate too because the track width and height are determined by deposited layer thickness and track mass m is different as laser power and scanning speed (or energy input) is changed. That is to say, track mass m is not a constant. So it is not a feasible way to discuss the relationship between energy input and material physical properties. However, formula $\psi_1 = 4p/\pi d^2 v$ will be more useful in practical use. Different researchers do their SLM experiments by using different types of lasers (laser model is generally TEM00) and different spot diameters. It can be useful to access whether the SLM apparatus can manufacture high density metal parts directly or not, by calculating if the ψ_1 can reach to the energy input level of the track of regular and thin shape mentioned above

Fig. 5 The relationship between scanning space and overlapping rate

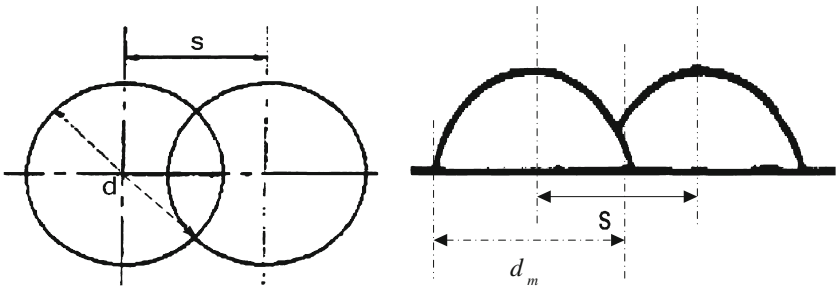

a $\phi = \frac{d-s}{d} \times 100\%$ b $\phi = \frac{d_m - s}{d_m} \times 100\%$

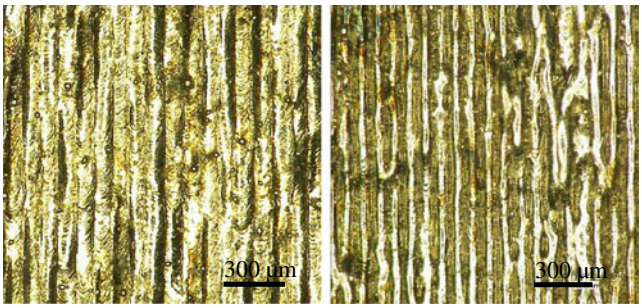

Overlapping rate 30% (scanning spacing 0.07mm) Overlapping rate 10% (scanning spacing 0.09mm)

Fig. 7 Different overlapping rates experiment of the shape regular and thin track

(the layer thickness in the formula (1) is not taken into account, because the layer thickness should be set as thin as possible according to the particle size.)

The track width is also an important reference factor for manufacturing, and it has great influence on the dimensional accuracy and surface roughness of the final fabricated parts. Figure 4 shows the influence of laser power density and scanning speed on the width of single track. It can be seen that the track width decreased as the laser power density decreased and scanning speed increased.

3.2 Multi track

3.2.1 Heat accumulation

Because of the overlapping during multi-track scanning, the already formed tracks will inevitable has heat effect on the next track, so energy density formula ψ_1 need to be changed to $\psi_2 = \frac{4P}{\pi d^2.v}(1+\varepsilon)$, ε is heat accumulation factor of multi-track; ε is closely related to overlapping rate. In addition, the just formed track provides a wetting matrix for the next track. Due to the above two reasons, the distribution of track shape shift to the lower right in Fig. 3, that is to say lower laser power or higher scanning speed will be fine when producing regular or continuous tracks.

3.2.2 Overlapping rate

In order to obtain dense and smooth surface, appropriate overlapping rate between tracks should be considered (not use the concept of scanning space, as the scanning space varies with the track width). The formula $\phi = \frac{d-s}{d} \times 100\%$ is mostly used to calculate overlapping rate during multi-track fabrication, just as Fig. 5a shows, s is scanning space, d is spot diameter. However, the formula above does not consider practical track width, which varies with laser processing parameters (laser power, scanning speed). Therefore, it is necessary to replace spot diameter d with practical track width d_m, and the formula can be changed to $\phi = \frac{d_m-s}{d_m} \times 100\%$, as Fig. 5b shows, scanning space s is preset, and practical track width d_m can be got according to Fig. 4.

According to single-track analysis, the regular- and thick-shape and regular- and thin-shaped tracks were suitable for SLM fabrication. During multi-track fabrication, regular- and thick-shaped track had a larger range of powder-free zone, making the next track not to have enough material and the volume become smaller. Therefore, large scanning spacing (low overlapping rate) should be adopted for the regular- and thick-shaped track. Figure 6 shows the multi-track surface morphology of regular- and thick-shaped track, overlapping rate respectively at 30% and 10%. It can be seen that the surface reaches an excessive molten degree when overlapping rate was 30%, also serious lack of metal material. The reason is partly due to laser remelting of the previous track; the other reason is the vaporization of the pool and the formed plasma will give a recoil pressure back to the pool, making the track spread out. However, when at 10% overlapping rate, it could clearly see the single track and the valley between adjacent tracks. Each track was still regular, continuous with less material loss in pool, making it appropriate for SLM fabrication. So for the regular- and thick-shaped track, low overlapping rate was required.

For the track of regular and thin shape, track width had decreased significantly, and powder around the pool had not been blown away; therefore, required a higher overlapping

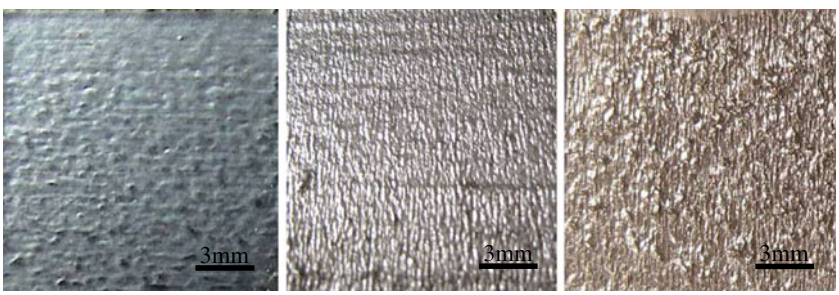

Fig. 8 Gradual deterioration of surface quality during SLM procession

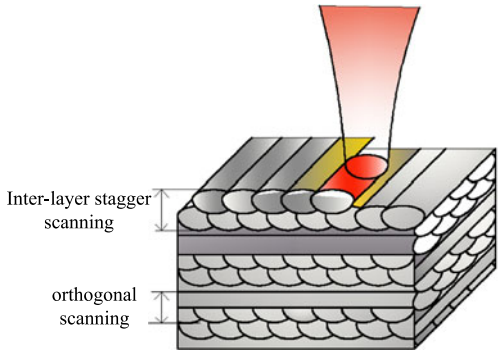

Fig. 9 Inter-layer stagger and then orthogonal scanning strategy

rate. Figure 7 shows the multi-track surface morphology of the regular- and thin-shaped track, overlapping rate was respectively at 30% and 10%. It can be seen when the overlapping rate was 10%, the tracks did not overlap closely to ensure the compactness of surface. Only when the overlapping rate was around 30% can it ensure strong overlapping between pools and forming a smooth surface. The reason can be explained that when overlapping rate was around 30%, the scanning spacing was approximately 70–80 μm, exactly the same size as focused spot diameter. The authors think this range of scanning spacing will ensure uniform distribution of energy during multi-track fabrication, not causing excessive residual stress and warping default.

It can be concluded from multi-track experiments that when the shape of regular- and thick-track employed low overlapping rate(say 10%), and the shape of regular and thin track employed a larger overlapping rate (say 30%), the multi-track surface will be fine, which provided the basis for selecting the overlapping rate during multi-layer fabrication. In the actual SLM processing, we should also consider: (1) processing efficiency, which is mainly related to scanning speed; (2) the residual stress accumulation caused by excessive heat input, which can easily lead to warping, crack, etc.; (3) the impurities generated by material vaporization in the chamber during manufacturing process will seriously pollute the optical lens. Therefore, it is believed that multi-layer experiment should be established on the basis of the shape of regular and thin track.

3.3 Multi-layer fabrication

3.3.1 Heat accumulation

Heat accumulation effect should not be ignored in multi-layer fabrication. The accumulated amount of heat warming up the subsequent layer, leading to less laser energy input requirements. During multi-layer fabrication, laser energy input formula (2)should be modified as [20]:

$$\psi_3 = \frac{4P}{\pi d^2.v}(1+\varepsilon_1) + E_a \tag{3}$$

In formula (3), E_a is the heat building-up value. E_a is related to P/v, scanning area of each layer and cooling rate. Heat accumulation makes the distribution of track types (Fig. 3) continue to shift to the lower right, so desired track (type 2) can be got by using lower laser power or higher scanning speed. The value of E_a will become larger as the number of stacked layers increase, only when the accumulated heat in one layer is equal to dissipated heat, the E_a will remain unchanged.

Fig. 10 SLM fabrication of 316 L stainless steel cubic part

Processing parameter	Value	
Laser power	150W	
Scanning speed	300mm/s	
Scanning line overlapping rate	30%	
Focused diameter	70～80μm	
Scanning strategy	Inter-layer stagger scanning strategy	
Layer thickness	35μm	
Oxygen content in chamber	<0.1%	
technical parameters		Cubic entity fabrication

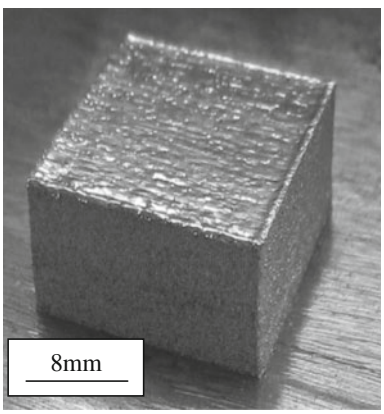

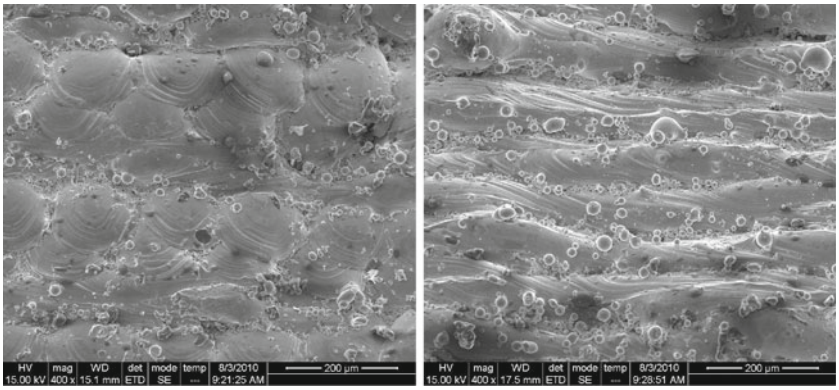

Fig. 11 Analysis of the sample's surface morphology

3.3.2 Surface deterioration

Multi-layer fabrication is much more difficult than single track or multi-track fabrication because the conditions are more complicated during multi-layer fabrication. Factors such as flatness of powder spreading, stability of effective laser power, and oxygen content in chamber are all critical to ensure fabrication stability. Even if the above conditions are strictly controlled, the fabricating part's surface will still deteriorate gradually. Figure 8 shows the morphology of first layer, 10th layer and 30th layer in a cube fabrication. The first layer was smooth and the 10th layer was slightly uneven but still fine, but the 30th layer surface had become very rough.

Surface quality deterioration leads to poor powder spreading effect, which results in rougher surface. It is believed that the pool solidification and shrinkage is the main reason for deterioration of surface quality. Assume a layer thickness is set to h, stainless steel powder density ρ_1 and fabricated part density ρ_2, the shrinkage of metal powder after melting and solidification approximately equal to $(1-\frac{\rho_1}{\rho_2})$, the nth layer thickness h_n can be expressed as follow:

$$\begin{aligned} h_2 &= h + h_1(1-\tfrac{\rho_1}{\rho_2}) \\ h_3 &= h + h_2(1-\tfrac{\rho_1}{\rho_2}) \\ &\cdots\cdots \\ h_n &= h + h_{n-1}(1-\tfrac{\rho_1}{\rho_2}) \end{aligned} \tag{4}$$

We can get the limit of h_n when n reaches to infinity, which means many layers have been fabricated (normally more than ten layers):

$$\lim_{n\to\infty} h_n = \lim_{n\to\infty} h\frac{1-(\frac{\rho_1}{\rho_2})^n}{1-\frac{\rho_1}{\rho_2}} = h\times\frac{1-0}{\frac{\rho_1}{\rho_2}} = h\times\frac{\rho_2}{\rho_1}$$

The above equal which proves the gradually increase of layer thickness, but the layer thickness increases towards a fixed value. Assume h=35 μm, ρ_1=4.04 gcm^{-3}, ρ_1=7.98$g.cm^{-3}$, the actual layer thickness will reaches up to 70 μm according to the above analysis. In the actual SLM manufacturing process, the gradually thickened layers could be observed. The thickened layer thickness increases the instability of the pool, and is unfavorable for the pool and the substrate combination. Thickened layers also increase the balling tendency, which is an important reason for surface deterioration.

In order to prevent deterioration of the surface as the result of the thickened layer, there are several effective ways to improve the surface quality, including (1) real-time adjustment of technical parameters during manufacturing. For example, increase in the scanning speed appropriately will gradually improve the surface quality, but accompanied by a slight decline in density. (2) Remelting of the deteriorated surface with special parameters. (3) Special scanning strategy can be used, such as the inter-layer stagger scanning strategy as described below.

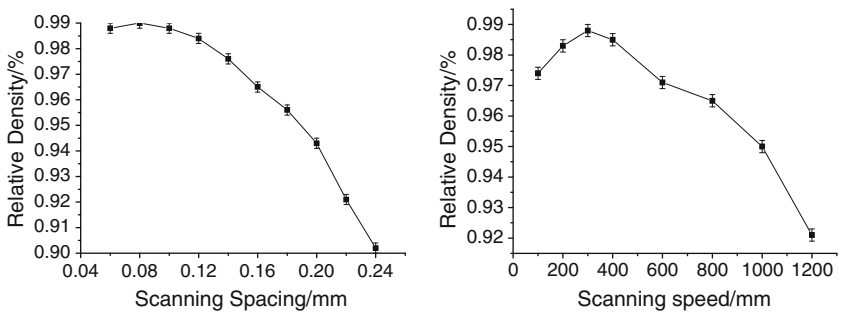

Fig. 12 The affect of scanning spacing and scanning speed on 316 L stainless steel part's density fabricated by SLM

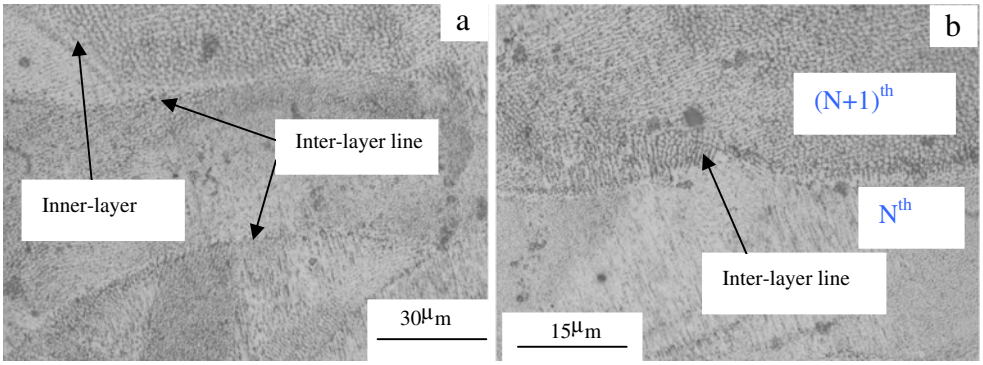

Fig. 13 Microstructure of 316 L stainless steel part produced by SLM

3.3.3 Scanning strategy

According to single-track and multi-track experimental analysis, the shape of molten pool after solidification is elliptical and micro-gully will be generated when tracks overlap together, such as the shape of regular and thick track of 10% overlapping rate has obvious gully. Generally, there will be more instability in track overlapping zones than in elsewhere. Gas holes and inclusions tend to form in the track overlapping zone. Some researchers had done in-depth and comprehensive study on SLM scanning strategy. Most studies concluded [16, 17] that more dense parts can be got by using inter-layer stagger scanning strategy (or called refill strategy). The main reason lies to that inter-layer scanning strategy can repair defects of previous layer by scanning at the track overlapping zone. In order to reduce the stress accumulated along the same direction in this experiment, orthogonal scanning and inter-layer stagger scanning strategy were combined together, which can be described as: the first two adjacent layers using inter-layer scanning strategy, and the next two adjacent layers were scanned still using inter-layer scanning strategy, but vertical to the previous two layers, as Fig. 9 shows.

3.3.4 Cubic part fabrication and surface analysis

Figure 10 shows the optimized parameters and a cubic part with side dimension of 15 mm manufactured by SLM.

Figure 11 shows the sample's side and upper surface morphology respectively, from which the compact overlapping effect between adjacent tracks and layers can be seen. Figure 11a shows the tracks arranged in staggered manner between adjacent layers, proving the inter-layer stagger scanning strategy used in experiment. From Fig. 11a, it can also be identified that the track overlapping rate is from 30% to 35%, just the same as the set value. There are some fine powder particles that were not melted adhered to the junctions of layers and tracks, which were mainly caused by the influence of laser heat effect. Figure 11b shows some inserts imbedded in the upper surface, the compositions of these inserts are mainly the oxide of Si, Ca, and Mn elements. The existence of oxides will affect the comprehensive properties of the parts. The reason for oxide formation may be attributed to the high oxygen content in the chamber or spattering that happened during the manufacturing.

Besides layer thickness, scanning spacing and speed are the most important two parameters affecting part's quality. Based on the cubic fabrication process parameters, Fig. 12 shows the relationship between scanning spacing, scanning speed, and the cubic density.

Figure 12a shows the part's density reaches more than 98% when the scanning spacing was in the range of 0.06–0.12 mm. The reason is that under the conditions of inter-layer stagger scanning strategy and scanning spacing was less than 0.12 mm, the track overlapping rate would be at least 30%. When the scanning spacing was bigger than 0.12 mm and increases, lower overlapping rate and more pores happen, and the density decreased from 98% to around 90% when scanning spacing increased from 0.12 to 0.24 mm. Figure 12b shows that when scanning speeds increased from 100 to 300 mm/s, the density did not decrease but increases. The reason may lie to low-speed scanning resulting in a powder-free zone around track, which leaded to material loss in pool. When the scanning

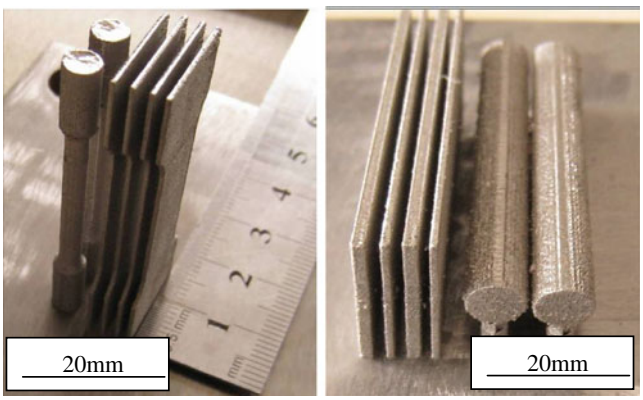

a fabrication perpendicular to tensile direction b fabrication parallel to tensile direction

Fig. 14 Mechanical properties testing samples fabricated by SLM process

Table 3 Comparison of mechanical properties, hardness between SLM parts and casting parts

Samples	Tensile strength (MPa)		Elongation (%)		Micro-hardness (HV)
	Stacked perpendicular to drawing direction	Stacked parallel to drawing direction	Stacked perpendicular to drawing direction	Stacked parallel to drawing direction	
Sample 1	636	532	35	15	265
Sample 2	624	561	31	19	258
Sample 3	582	554	29	22	270
Casting	>480		39		>220

speed was greater than 300 mm/s, the density began to decrease, as scanning speed increased to 1,200 mm/s, the density decreased to 90%.

3.3.5 Microstructure and mechanical properties

The microstructure of SLM part is different from the traditional cast parts. As the laser beam moves ahead, heat conduction direction is perpendicular to the solidification front, also to the surrounding layers and previous solidified layer, which leads to multidirections grain growth. At the same time, the SLM process is a high-speed solidification process leading to formation of large number of grains simultaneously, so the neighboring grains meet and contact soon. As a result, the grains are very small and microstructure is fine. Figure 13 shows the SLM 316 L stainless steel part's micro-structure observed perpendicular to scanning direction, which was mainly composed of equiaxed grains and columnar crystal, and it could also be seen that the grains had diversified growing direction. The grain sizes measured at about 1–2 μm or even submicron.

Mechanical properties test samples manufactured by SLM were designed according to GB-T 228–2002 as shown in Figure 14. The measured results in Table 3 shows that SLM fabricated parts' tensile strength was significantly higher than casting. When stacked along the direction perpendicular to the tensile direction, the parts' tensile strength was 20–30% higher than casting, and elongation was slightly lower than the casting. When stacked along the direction parallel to the tensile direction, the part's tensile strength was 10–15% higher than casting, and elongation was 40–50% lower than casting. Microhardness tests show that SLM fabricated part's hardness was higher than the casting parts. The main reason was related to rapid solidification characteristics during SLM process.

3.3.6 SLM fabrication with sample applications

Compared to traditional manufacturing process, SLM method for direct manufacturing of end-use products has advantages of (1) not subjected to restrictions of geometry complexity and (2) direct access to high-density parts with metallurgical bonding structure. When using the SLM method to manufacture parts, quality requirements, the volume and shape of the part's complexity should be considered. Quality requirements determine whether the SLM technology will meet the actual demand, and the size and shape of the part determine the manufacturing cost. The SLM method is suitable for products that have no requirement of fine surface quality, for small-batch production and for small parts with complex structure. Some SLM fabricated examples are given in Fig. 15, where curved surface gear (Fig. 15a) and electronic products for heat dissipation (Fig. 15b) are shown.

4 Conclusions

Four different track types were obtained at different energy input, including regular and thick shape, regular and thin

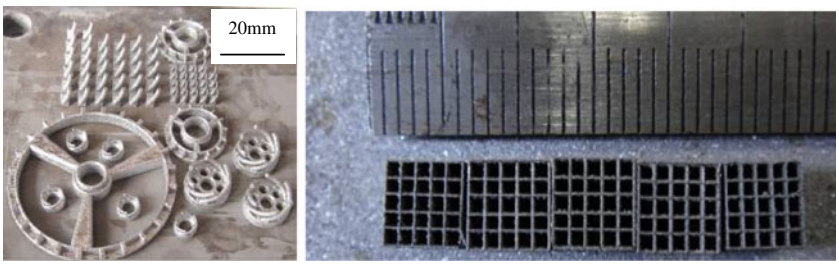

(a) new gear with curved surface (b) heat dissipation in electronic products

Fig. 15 SLM fabricated samples

shape, regular but occasionally broken shape, irregular and pre-balling shape. Considering fabrication efficiency and stability, the shape of regular and thin track was considered more desirable for SLM fabrication with overlapping rate of around 30%. As a result of the heat accumulation, the distribution of track shape would slowly shift to the lower right in multi-track and multi-layer fabrication, that is to say, lower laser power or higher scanning speed was all right to get the shape of regular and thin track. Layer thickness will gradually become thick, leading to deterioration of the surface. The inter-layer staggered scanning strategy helped reduce porosity and improve the bonding strength for multi-layer fabrication. By testing the 316 L stainless steel samples fabricated by SLM process, it could be found that the microstructure was composed of fine equiaxed and columnar grains. The tensile strength and hardness of 316 L stainless steel fabricated by SLM method were higher than casting parts, but elongation was lower. The experiments proved that 316 L stainless steel part with smooth surface could be directly produced by SLM process, which would be suitable for a wide range of applications in medicine, moldmaking, and automotive industry.

Acknowledgment The work described in this paper was fully supported by a project from Industry, University and Research Institute Combination of Ministry of Education, Science and Technology and Guangdong Province, China (Project No. 2010A090200072)

References

1. Electro Optical Systems Website. *e-Manufacturing Applications*, http://www.eos.info/en/applications.html. Accessed on October 2010
2. RERLIZER^{SLM} Website. *SLM^{TM} in Action*, http://www.realizer.com/en/startseite/slm-in-action. Accessed on June 2010
3. CONCEPTLASER Website. *Industry*, http://www.concept-laser.de. Accessed on May 2010
4. Arcam Website. *Industry Segments*, http://www.arcam.com/industry-segments/index.aspx. Accessed on July 2010
5. Santos EC, Shiomi M, Osakada K, Laoui T (2006) Rapid manufacturing of metal components by laser forming. Mach Tools Manu 46(13):1459–1468
6. Yadroitsev I, Shishkovsky I, Bertrand P, Smurov I (2009) Manufacturing of fine-structured 3D porous filter elements by selective laser melting. Appl Surf Sci 255(10):5523–5527
7. Hao L, Dadbakhsh S, Seaman O, Felstead M (2009) Selective laser melting of a stainless steel and hydroxyapatite composite for load-bearing implant development. J Mater Process Tech 209 (17):5793–5801
8. Childs THC, Hauser C, Badrossamay M (2005) Selective laser sintering (melting) of stainless and tool steel powders: experiments and modeling. Proceedings of the Institution of Mechanical Engineers, Part B: J Eng Manu 219(B4):339–358
9. Kruth JP, Froyen L, Vaerenbergh JV, Mercelis P, Rombouts M, Lauwers B (2004) Selective laser melting of iron-based powder. J Mater Process Technol 149(1–3):616–622
10. Murr LE, Quinones SA, Gaytan SM, Lope MI, Podela A, Martinez EY, Hernandez DH, Martinez E, Median F, Wicker RB (2009) Microstructure and mechanical behavior of Ti-6Al-4 V produced by rapid-layer manufacturing, for biomedical applications. J Mech Behav Biomed Mater 2(1):20–32
11. Yadroitsev I, Bertrand P, Smurov I (2007) Parametric analysis of the selective laser melting process. Appl Surf Sci 253(19):8064–8069
12. Yadroitsev I, Thivillon L, Bertrand P, Smurov I (2007) Strategy of manufacturing components with designed internal structure by selective laser melting of metallic powder. Applied Surface Scicence 254(4):980–983
13. MumtaZ KA, Erasenthiran P, Hopkinson N (2008) High density selective laser melting of Waspaloy. J Mater Process Technol 195 (1–3):77–87
14. Wong M, Owen I, Sutcliffe CJ, Puri A (2009) Convective heat transfer and pressure losses across novel heat sinks fabricated by selective laser melting. Int J Heat Mass Trans 52(1–2):281–288
15. Yadroitsev I, Bertrand P, Laget B, Smurov I (2007) Application of laser assisted technologies for fabrication of functionally graded coatings and objects for the international thermonuclear experimental reactor components. J Nucl Mater 362(2–3):189–196
16. Beal VE, Erasenthiran P, Hopkinson N, Dickens P, Ahrens CH (2006) The effect of scanning strategy on laser fusion of functionally graded H13/Cu materials. Int J Adv Manuf Technol 30(9):844–852
17. Li RD, Shi YS, Liu JH, Xie Z, Wang ZG (2009) Selective laser melting W-10 wt.% Cu composite powders. Int J Adv Manuf Technol 48(5–8):597–605
18. Morgan R, Papworth AJ, Sutcliffe C, Fox P, Neill WO (2002) High density net shape components by direct laser re-melting of single-phase powders. J Mater Sci 37(15):3093–3100
19. Simchi A (2006) Direct laser sintering of metal powders: mechanism, kinetics and microstructural features. Mater Sci Eng 428(2):148–158
20. Ning Y, Wong YS, Fuh JYH, Loh HT (2006) An approach to minimize build errors in direct metal laser sintering. IEEE Transactions on Automation Science And Engineering 3(1):73–80